ELSEVIER

Catalysis Today 77 (2003) 407–417

CATALYSIS TODAY

www.elsevier.com/locate/cattod

The use of temperature-programmed and dynamic/transient methods in catalysis: characterization of ceria-based, model three-way catalysts

Marta Boaro[1], Michela Vicario, Carla de Leitenburg, Giuliano Dolcetti, Alessandro Trovarelli*

Dipartimento di Scienze e Tecnologie Chimiche, Università di Udine, via Cotonificio 108, 33100 Udine, Italy

Abstract

Temperature-programmed (TP) methods have been increasingly used in recent years for the characterization of catalytic materials under conditions similar to those encountered in commercial applications. A large variety of complementary TP techniques can be used with minimum variation of experimental conditions, thus allowing great characterization potential in a single apparatus. Modern analytical and numerical tools allow accurate analysis and modeling of TP profiles, to obtain kinetic and other reaction parameters. Here, we will briefly review the experimental TP methods used for the characterization of the reduction features and the dynamic behavior of oxygen-storage/redox components of auto exhaust catalysts, based mainly on CeO_2 and ceria-zirconia.

Keywords: Temperature-programmed and dynamic/transient methods; Catalysis; Three-way catalysts; TPR; Ceria; CeO2; Oxygen storage

1. Introduction

The interest in temperature-programmed (TP) and transient methods in heterogeneous catalysis has experienced rapid growth in recent years. This attention is motivated by a number of factors, including the development of experimental techniques for monitoring concentration in the gas phase with a sensitivity and time-resolution not previously available; the recognition that simple experiments can quite often give a quick answer to catalytic performances of materials under conditions close to those encountered in industrial operation; and the availability of efficient numerical methods to model and predict the dynamics of complex reaction systems under transient and TP methods.

The interaction of reactants with the catalyst surface is a key parameter in heterogeneous reaction systems. For example, the temperature at which species are desorbed from a surface is indicative of the strength of the surface bond: the higher the temperature, the stronger the bond. Therefore the adsorption of a probe molecule at low temperature, and subsequent monitoring of its desorption/reaction characteristics with temperature, is a simple way to characterize surface properties of catalysts and adsorbents. This is the basis of TP analysis methods in which, for a linear increase in temperature, the concentration of the reacting/desorbing

* Corresponding author.
E-mail address: trovarelli@dstc.uniud.it (A. Trovarelli).
[1] Present address: Chemical Engineering Department, University of Pennsylvania, 220 South 33rd Street, Philadelphia, PA 19104, USA.

0920-5861/02/$ – see front matter
PII: S0920-5861(02)00383-8

particles is recorded as a function of temperature.

These methods have been widely applied to industrial catalysts primarily because their conditions of use are close to those encountered in commercial operations. In addition, the transient nature of a TP analysis technique, in which the temperature, the surface coverage and the reaction rate all vary with time, has the advantage of providing information not available from steady-state experiments.

Several different applications of TP methods have been employed in recent years and have been detailed in excellent reviews [1–4]. In this paper, a few of the basic concepts underpinning these techniques will be given and one case of study will be presented.

2. Generality of TP methods

Based on similarity of experimental procedure, TP methods for the characterization of catalysts can be classified in a very broad range of techniques known as thermoanalytical techniques [3]. Table 1 presents a classification of these techniques. Strictly speaking, TP methods in catalysis research include those belonging to classes 4 and 5, i.e. TP desorption and TP reaction although the TP methods represented in the other classes have also been profitably applied. The former can give information on the physical desorption of gases as well as on gases evolved by chemical mechanisms while the latter includes several possibilities and is identified as a more chemical-based technique concerned with analysis of gases from purely chemical processes. To this class belong the majority of TP methods. In temperature-programmed reduction (TPR), the reduction of a solid is carried out with diluted H_2 and at the same time the temperature of the system is linearly increased. Similarly, temperature-programmed oxidation (TPO) utilizes diluted oxygen to oxidize a solid material (a reduced phase or supported metals or deposited carbon) as a function of temperature. Temperature-programmed (surface) reaction (TPSR, TPRe) refers to the study of reactions under TP conditions. This type of study can be conducted in two different ways: (i) the reagents (usually two gases) can be coadsorbed on the catalyst and heating done in an inert carrier; or (ii) a carrier gas containing reagents can be used and reaction carried out by increasing temperature. Since several sites of different activity can exist on the catalyst surface, which can increase or decrease with a change in catalyst temperature, this approach permits the evaluation of kinetic parameters and activity data at various temperatures and the monitoring of the contribution of each site to catalytic activity. Specifically, depending on the type of reaction carried out, we may refer to TP hydrogenation, methanation, sulphidation, combustion, carburization, gasification, etc.

The majority of information can be obtained by a simple qualitative approach which does not require modeling. The comparison of different profiles with “calibrated profiles” and/or the evaluation of specific parameters in a sequence of profiles (temperature of maximum, number of peaks, peak area, etc.) is more often sufficient for the characterization of the system under investigation.

The analysis is most often confined to a qualitative level by discussion of peak maxima, number and position of peaks, and total reactant consumption. However, if a more detailed picture is required, several theoretical models have been developed especially for TPD and TPR analysis (see, e.g., [5–9]).

Table 1
A classification of TP techniques [3]

Thermoanalytical techniques	
Techniques dependent on dimensional changes	Dilatometry
Techniques dependent on weight changes	Thermogravimetry
Techniques dependent on energy changes	Differential thermal analysis (DTA), differential scanning calorimetry (DSC)
Techniques dependent on evolved gas analysis	TP desorption
Techniques dependent on gas analysis from chemical reaction	TPR, TPO, temperature-programmed (surface) reaction

3. Experimental methods

Several experimental setups have been used and described for carrying out TP desorption and reaction/reduction studies. Only the simplest arrangement will be discussed here. It can be used for both desorption and reaction studies. It is generally composed of three main sections: (1) Introduction of reactants; (2) Furnace and reactor; and (3) Detector and data-acquisition system.

The gas introduction section consists of a series of valves and mass-flow controllers which allow for adsorption of various components and regulate the carrier/reacting gas stream fed to the reactor during heating. Generally, the carrier gas is He or Ar, although N_2 can also be used. In the last case, however, if a mass spectrometer (MS) is used for detection, mass 28 corresponding to CO cannot be observed. The composition fed to the reactor depends on the type of experiment. For TPR, a composition of H_2 1–10% in Ar or He is generally used. TPO requires 1% oxygen in He while for TPD, pure He is preferred. Other TP reaction techniques require a feed composition which depends on the specific reaction carried out. Thus for TP methanation, CO can be adsorbed on the catalyst and heating carried out with H_2/He reacting carrier, or CO/H_2 can be used directly in the carrier gas.

The furnace is generally of the vertical tubular type and must be able to maintain a linear temperature rise to at least 1273 K for high-temperature studies. Heating is generally controlled by a PID temperature programmer and typical heating rates range from 2 to 30 K/min. The reactor is inserted into the furnace. It consists of a quartz tube (Φint. 6–12 mm) designed to properly hold the catalyst. A thermocouple is inserted into the catalyst bed to monitor catalyst temperature. The amount of catalyst loaded can be in the range from 50 to 300 mg with a flow rate of 20–200 ml/min.

The detector is the most important part of the system. Two types of detectors can be used: a thermal conductivity detector (TCD) without or with a separating column or a quadrupole MS. TCD with a separating column, that is a gas chromatograph, can be used when more than one desorbed gas is present and it has the advantage of giving an accurate quantification of gases evolved during analysis. However, its most significant drawback is that measurements cannot be carried out continuously because of separation times. This results in very poor time-resolution of TP profiles. Recently, with the introduction of micro GC which perform complex analysis in a few seconds this problem can be overcome and quantification of complex mixtures can be performed in the time interval required for TP analysis.

TCD without separation column can be used when only one component is present in the carrier gas. It is generally utilized for TPR and TPO analysis when only H_2 or O_2 is monitored, provided that cold traps are installed before the detector to eliminate water.

MS is most often used as a detector. It has the advantage of giving the concentration of a selected component continuously as a function of time. With the use of recently developed software, several components can be calibrated and quantified simultaneously. MS has also the advantage of giving an immediate response to leaks and impurities present in the system. Connection to the reactor can be made using a heated capillary which allows continuous sampling from atmospheric pressure to 10^{-7} Torr and minimal problems associated with mass selection during sampling. The main drawback is that it is the most expensive of the detection methods available. The acquisition data system is generally adapted from the software controlling the detector and it is necessary to display data in the form of concentration against temperature.

We will briefly discuss features of a typical apparatus used in our laboratory for combined TPD/TPR/TPO studies. A schematic diagram is presented in Fig. 1. In this scheme, a series of two six-way, two-position valves (V1–V2) allows the introduction of different streams to the reactor coming from three different stainless steel lines made with 1/8 in. tubes. Line (L1) is connected to treatment gases (reducing/oxidizing mixtures) to permit sample pretreatment in various atmospheres. It is in fact necessary to treat the sample before analysis to eliminate adsorbed molecules which could otherwise affect TP analysis. Line (L2) is the line connected to reaction and carrier gases, which can be H_2/He, O_2/He or He for TPR/TPO and TPD analysis. Line 3 is connected to adsorbing gases. These gases are fed to a sampling loop (10–500 μl) in valve V1 which can be used to inject the mixture to the reactor. A separate external line L4 is used for calibration purposes with standard mixture. The analytical system consists of an MS and a micro GC which analyze simultaneously gases

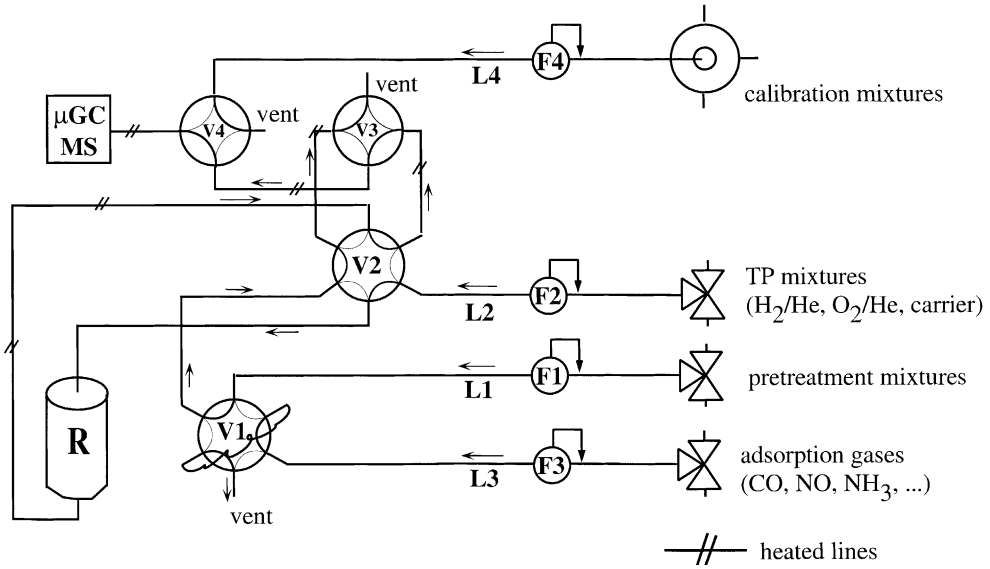

Fig. 1. Schematic diagram of an apparatus for TP analysis. F1–F4 mass-flow controllers, V1–V2 six-way two-position valves, V3–V4 four-way two-position valves, *R* reactor.

evolved from the reactor. To avoid dilution of peaks and time lag between reaction and detection, downstream the reactor the lines are 1/16 in. in diameter.

4. A case of study: investigation of oxygen-storage phenomena in ceria-based catalysts with TP techniques

In this section, we will briefly review some applications of TP techniques to the characterization of the oxygen-storage properties of auto exhaust catalysts. Three-way catalysis is the current technology used for abating emissions from internal combustion engines [10]. The catalyst is composed of a carrier material, mainly γ-Al_2O_3, stabilized with La_2O_3, Ba, etc., a catalytic active phase (precious metals like Pt, Pd, Rh) and an oxygen-storage promoter which plays an important role in providing oxygen buffering capacity during the rich/lean perturbations of exhaust gases associated with the feedback control system. Under working conditions, the catalyst is in fact exposed to constantly varying feedstream compositions going alternately from rich exhaust stoichiometry (deficient O_2) to lean stoichiometry (excess O_2). In this environment, the promoter has the ability to donate its oxygen for the removal of CO and hydrocarbons (HC) during the oxygen-deficient portion of the cycle while adsorbing and storing oxygen from O_2, NO and water during excursion into the lean part of the cycle. These reactions positively affect the conversion of the three major pollutants (CO, HC and NO) under conditions typically encountered in the normal operation of a three-way catalyst. This unique feature is carried out in commercial catalysts by cerium dioxide and CeO_2-based promoters. The use of these materials derives from the ability of CeO_2 to be *easily* and *reversibly* reduced to several CeO_{2-x} stoichiometries when exposed to O_2-deficient atmospheres [11,12].

4.1. TPD studies

The role of ceria in providing oxygen for CO oxidation and capturing oxygen from NO decomposition can be satisfactorily evidenced by TP desorption studies [13,14]. Fig. 2 shows a series of successive TPDs of adsorbed NO on reduced Pt/Al_2O_3 and $Pt/CeO_2/Al_2O_3$ catalysts. The signal of N_2 is recorded during linear heating after adsorption of NO at room temperature. Experiment 1 is obtained with reduced samples while successive adsorption and desorption runs were carried out without further

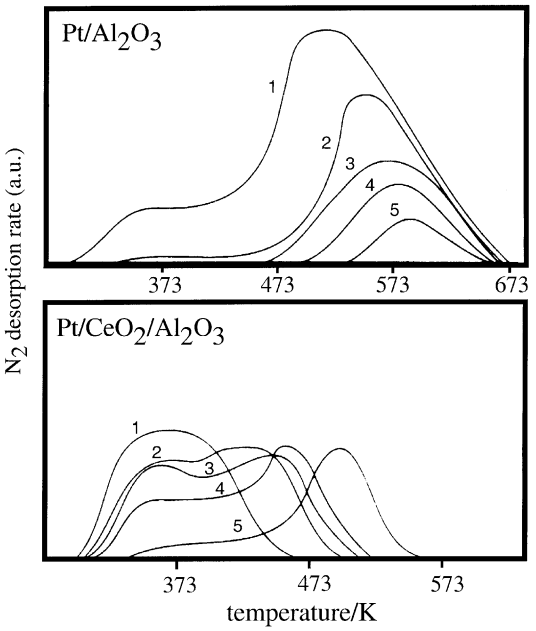

Fig. 2. TPD of NO over Pt/alumina and Pt/ceria-alumina [13].

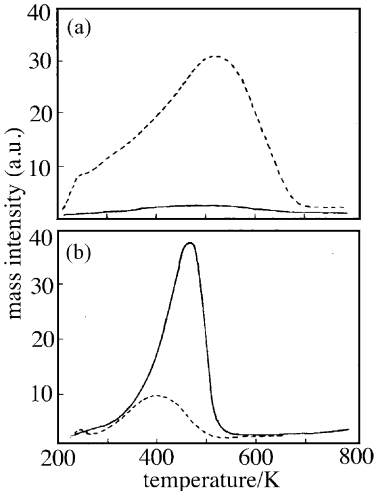

Fig. 3. TPD of CO over reduced (a) and oxidized (b) Pd/CeO_2 [14]. Mass 28 (- - -); mass 44 (—).

reduction. Only very weak or no desorption of NO and N_2O were observed in experiment 1, evidencing that the decomposition of NO via $2NO = N_2 + O_2$ occurs predominantly on freshly reduced samples. It is shown that with Pt/Al_2O_3, NO decomposition becomes incomplete in successive cycles (cycles 2–5), demonstrating that oxygen atoms deposited after each run inhibit the capacity of the catalyst to decompose NO. The addition of ceria has a dramatic effect on TPD desorption spectra: (i) the main desorption peak is located at 373 K, ca. 150 K lower than that observed on Pt/Al_2O_3; (ii) as successive runs are performed and oxygen is accumulated on the catalysts, the main N_2 desorption peak moves to a higher temperature close to that observed when ceria is not present; and (iii) the oxygen-inhibiting effect is much lower. This can be explained by the ability of ceria to attenuate the negative effect of oxidizing atmospheres by temporarily storing oxygen in the lattice. The noble metal does play an important role in this mechanism by providing a kinetic path for gas-phase oxygen to reach ceria (some kind of oxygen spillover effect).

On oxidized support, that is when ceria is in the form of CeO_{2-x} with x close to 0, oxygen from the lattice can be available for oxidation in the absence of gas-phase oxygen. TPD of CO adsorbed on reduced and oxidized Pd/ceria clearly highlight this point by showing no CO_2 desorption in the former case and enhanced CO_2 formation in the latter case (Fig. 3). This can be attributed to direct reaction of CO with lattice oxygen, forming an oxygen vacancy $CO + O_L = CO_2 + V$. This process can also be evidenced by CO TPR. In this case, a mixture of CO/He is used as a reducing agent. It is passed over pure ceria while temperature is linearly increased. CO_2 formation rate reaches a maximum at around ca. 830 K as the result of reduction of ceria operated by CO [15].

4.2. TPR studies

H_2-TPR is also a convenient way to investigate the reduction/oxygen-storage properties of CeO_2 for application in TWCs. It gives information on the steps involved in reduction processes and is very sensitive to changes in textural, morphological and structural properties of the oxide. Thus, TPR of ceria can be profitably used for characterization of pure and doped ceria, noble metals supported on ceria and associated effects (spillover, metal/support interaction), ceria supported on Al_2O_3, and mixed oxide-containing ceria.

The first TPR on ceria dates back to 1980 [16] but only a few years later was it first suggested that reduction of ceria may follow a two-stage process [17].

Typically, the reduction profile of ceria shows two peaks. The first low temperature signal located at ca. 770 K is assigned to the reduction of the most easily reducible surface-capping oxygen of ceria while removal of the bulk oxygen was suggested as the cause of the high-temperature signal at ca. 1100 K. Similar correlation were reported later by others, who found a good relationship between BET surface area and H_2 consumption from TPR at low temperature [18]. The presence of noble metals strongly modifies these features due to hydrogen activation by the metal and consequent migration to the support (spillover) favoring reduction of the ceria surface at lower temperature [19–21]. The TPR profile is modified by a shift of the low temperature peak of ceria reduction to lower temperature where reduction of the supported metal occurs. Fig. 4 shows the typical TPR profile of pure ceria and Rh/CeO_2 sample where it is shown the disappearance of the H_2 consumption peak at ca. 800 K and the appearance of a new peak at low temperature due to metal oxide and surface ceria reduction. The consequence is that in the presence of a noble metal, reduction of surface Ce(IV) is enhanced at lower temperature. An estimation of the reduction of ceria at low temperature in the presence of noble metals were carried out by de Leitenburg et al. [21] and the results are summarized in Table 2.

Recently the interpretation of ceria reduction peaks in TPR profiles, as due to surface and bulk reduction, has been critically revised and a quantitative model for ceria reduction during TPR has been reported [22,23]. From oxygen diffusion data it was concluded that oxygen diffusion can be neglected in modeling TPR

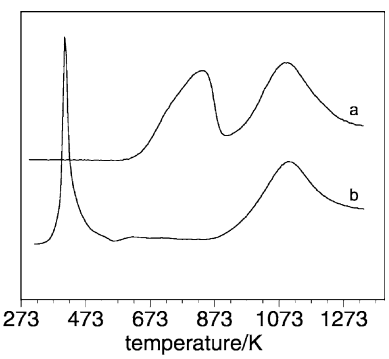

Fig. 4. TPR of pure CeO_2 (Grace Davison, surface area ca. 55 m^2/g) and Rh_2O_3 supported on same CeO_2.

Table 2
Degree of reduction of ceria at 500 K under TPR conditions [21]

Sample	x in CeO_x
CeO_2	2.00
Rh/CeO_2	1.95
Ir/CeO_2	1.97
Ru/CeO_2	1.95
Pt/CeO_2	1.96
Pd/CeO_2	1.96

experiments. Other factors were considered important like the variation of the thermodynamic reduction properties of ceria microcrystals as a function of their size and the textural changes occurring upon heating. Based on these factors the authors developed a simple kinetic model able to predict the unimodal and bimodal shape of low (LSA) and high surface area (HSA) ceria with correct location of the main peaks.

A few years ago, modified ceria catalysts were introduced in TWC formulations. They are based on ZrO_2 in the form of solid solutions with CeO_2 and characterized by an enhanced oxygen-storage capacity and thermal resistance compared to their ZrO_2-free counterpart [24]. TPR has been widely used initially to characterize the oxygen-storage/release behavior of these materials. Fig. 5 shows clearly that the introduction of ZrO_2 strongly modifies the reduction behavior of CeO_2 by shifting main H_2 consumption to a lower temperature [25]. By quantifying reduction according to the following equation:

$$Ce_xZr_{1-x}O_2 + \delta H_2 \leftrightarrow Ce_xZr_{1-x}O_{2-\delta} + \delta H_2O + \delta V_0$$

it is shown also that the value of δ varies with composition, reaching a maximum at around 50 mol% of the two oxides and is almost independent of surface area. The promotion of reduction is attributed to the enhanced oxygen mobility of solid solutions compared to pure oxides [24].

There are several points that still need to be considered in the interpretation of TPR diagrams, especially when H_2 consumption is monitored through TCD. One problem is associated with the non-specific nature of the detector which is also sensible to desorption of carbonates in the form of CO/CO_2 or methane [26]. It is therefore important that a cleaning procedure is adopted before any TPR measurement. This is

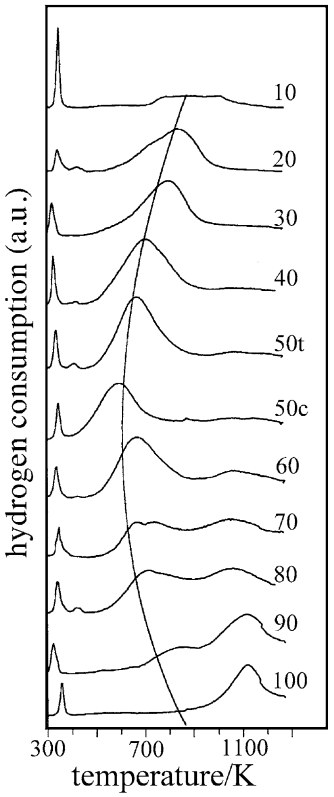

Fig. 5. Series of TPR of Rh/CeO_2–ZrO_2 at various compositions [25]. The molar content of CeO_2 is indicated on the right. For the 50:50 sample c and t indicate cubic and tetragonal phase, respectively.

generally made through an in situ oxidizing treatment [27] which also has the advantage of standardize the sample treatment procedure and in mixed valence materials, like ceria and ceria-based mixed oxides, to provide a uniform and reproducible redox state before analysis.

The major drawback to the application of conventional TPR to study reduction of cerium-based materials is due to the complex interaction of H_2 with ceria. The study of reduction of ceria and its interaction with hydrogen under more or less severe conditions has represented a major effort in the last decade and the main results have been critically reviewed in a number of recent surveys [28,29]. In short, the main findings can be summarized as follows: (i) ceria can be reduced by hydrogen at temperatures higher than 600 K, and its reduction is strongly affected by textural and morphological properties [22,30–32], nanocrystalline ceria being reduced more easily than bulk-like large ceria crystals [33]; (ii) irreversible and reversible reduction (i.e. reduction with and without water/vacancy formation) have been observed to occur depending on several variables like pre-treatments, precursor salts, presence of noble metals, etc. [28,34]; (iii) the presence of noble metal dramatically changes the redox behavior due to hydrogen activation by the metal at lower temperature and consequent migration to the support favoring reduction of the surface, the so-called H_2-spillover effect [19–21]; and (iv) incorporation of hydrogen by ceria during reduction has been reported to occur although this phenomena has given rise to discussion and controversy in the literature [18,30,35–38]. Therefore, it is clear that hydrogen consumption and vacancy formation cannot be simply related and the amount of the former can be much larger than that of vacancy formation.

Technical limitations of conventional TPR technique arise from the lack of quantitative data regarding H_2O production during reduction. This does not allow to distinguish if H_2 consumption originates from irreversible reduction and/or reversible reduction or adsorption/incorporation processes. The use of an MS detector, partly overcome these limitations and semi-quantitative data can be obtained [39]. However, the lower sensitivity and some dilution and mass selection effects can often be observed during capillary sampling, which does not allow precise quantitative analysis of peak shape and position. To allow a more precise quantitative monitoring of effluents and lack of mass-selection effect during sampling we have recently described a modification of the standard TPR apparatus with the introduction of a micro-GC detector which allows complete analysis of effluents (including CO and CO_2 originating from carbonate impurities) in approximately 1 min [40]; thus allowing a complete TPR profile to be collected in the range 298–1273 K with an accuracy of approximately 10 K in the determination of peak position. A comparison between the quantity and position of H_2 consumption and H_2O evolution peaks enables distinction between the type and extent of reduction and of any H_2 incorporation/spillover phenomena. As an example Fig. 6 shows a series of TPR carried out on Rh_2O_3 and CuO supported on ceria-zirconia. It is clearly seen that in the first TPR profile H_2 consumption is not “in phase” with water evolution, peaking at lower temperature.

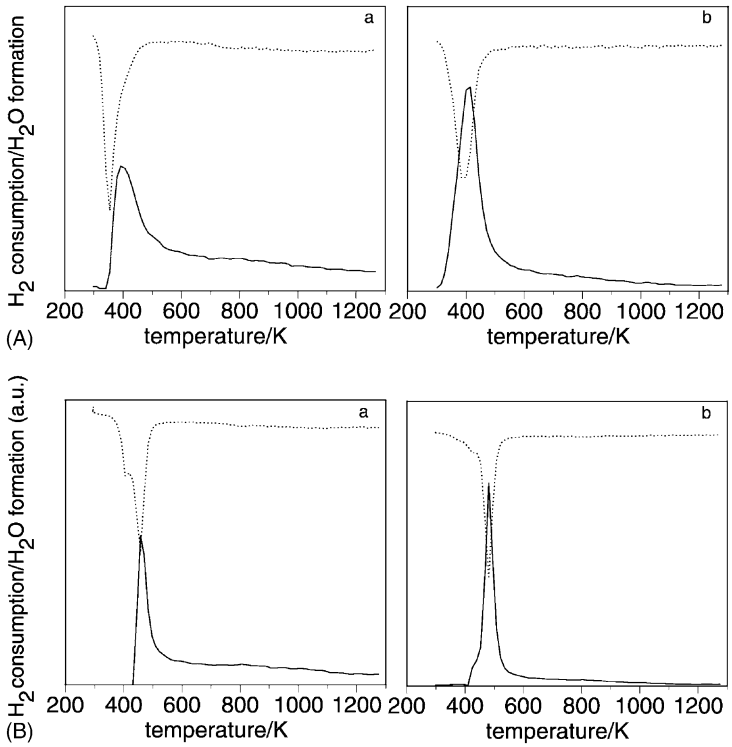

Fig. 6. (A) Profiles of H_2 uptake (dotted line) and H_2O evolution (solid line) obtained in TPR of (a) fresh $Rh_2O_3/Ce_{0.44}Zr_{0.56}O_2$ and (b) sample resulting from experiment a further reoxidized at 773 K. (B) Profiles of H_2 uptake (dotted line) and H_2O evolution (solid line) obtained in TPR of (a) fresh $CuO/Ce_{0.44}Zr_{0.56}O_2$ and (b) sample resulting from experiment a further reoxidized at 773 K.

Similar features were also observed with Pd and Au-based catalysts. This can be interpreted as an "hydrogen storage" phenomena in which hydrogen is initially utilized for rhodium and copper oxide reduction, then stored in some form on the support to be used for its reduction at higher temperature. It is not clear in which form hydrogen is stored on ceria but several possibilities exist, like formation of hydrides, hydroxyls, etc. [28,29,41]. A quantitative evaluation of water produced during reduction is in agreement with hydrogen consumed during the entire TPR, thus excluding any major phenomena of H_2 incorporation into CeO_2 lattice at the end of TPR experiments. The second TPR collected from samples resulting from first TPR further reoxidized at 773 K (Fig. 6, TPR b) does not show discrepancy in the positions of peaks due to hydrogen consumption and water evolution due to the lower surface area of sample after redox cycle which should hinder any H_2-storage/spillover phenomena [20]. A similar hydrogen storage effect was recently observed on Rh supported on ceria-silica [40], ceria-zirconia [39] and Cu on ceria [42]. In the latter case, the shift in peak position between H_2 and H_2O was associated to hydrogen adsorption prior to metal-oxide reduction.

4.3. Dynamic OSC studies

Overall, by carefully monitoring reduction behavior with TPR, we can obtain qualitative and quantitative information on the degree of reduction and the reduction rate as a function of temperature. In particular, the degree of reduction is easily obtained by integration of the TPR profile using a standard calibration, and better relates with the amount of oxygen thermodynamically available at a given temperature, what is generally called "total" oxygen storage capacity. However, great care should be used to directly correlate TPR data with the so-called "fast" or "kinetic" oxygen-storage

capacity. Although TPR data may be useful to rapidly evaluate the potential OSC of candidate materials, a definitive answer must be obtained from dynamic OSC measurements [27]. The amount of oxygen transferred in a dynamic regime better simulates the oscillations that the exhaust gas may undergo during real operation and is therefore much more useful in the evaluation of the activity of the material. This is therefore the oxygen that is kinetically available during the fast transitions between reduction and oxidation environments. Dynamic OSC measurements have been recently developed in combination with conventional TPR studies to offer a more appropriate characterization of the transient aspects involved in oxygen exchange during redox catalysis [27,43–49].

To better quantify the kinetically available oxygen during operation, we have recently developed in our laboratory a microreactor system working under TP dynamic reaction mode (for experimental details see [50]). The catalyst is exposed to an oscillating reducing/oxidizing mixture while temperature is linearly increased and from the response of the catalyst the OSC is evaluated. Specifically, we have studied the dynamic of CO oxidation over fresh and high-temperature-aged ceria-zirconia solid solutions with fast cycling feedstream composition. A constant gaseous flow of variable cycling composition was passed through the catalyst at a GHSV of approximately 150 000 h^{-1}. The composition cycle fed into the reactor consisted of CO and O_2, alternating with He with a frequency of 0.2–1 Hz. The reactants and CO_2 produced are measured against temperature in a sort of *TP dynamic reaction study* and the light-off temperature was assumed as a measure of the activity of the different catalysts. Fig. 7 shows the appearance of a typical TP dynamic CO oxidation profile. For clarity, only CO and CO_2 signals are reported. In this case, the temperature was linearly increased at a rate of 10 K/min while the concentration of reactants and product was constantly monitored by an MS. It may be clearly seen that CO_2 formation is the result of two distinct contributions (indicated as 1 and 2 in the inset of Fig. 7) whose relative intensity is dependent on temperature. The intensity of the first component generally increases with temperature, before reaching a steady-state value, while CO_2 originating from the second component shows a maximum of intensity at a conversion of ca. 50% and then slightly decreases. The dynamic of reactions con-

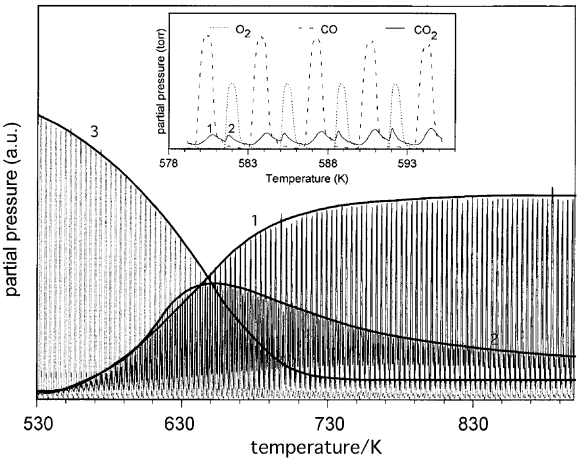

Fig. 7. TP CO oxidation under oscillating environment over $Ce_{0.5}Zr_{0.5}O_2$. Peaks indicated with 1 and 2 refer to signal at *m*/*e* 44, while 3 refer to *m*/*e* 28. For clarity oxygen signal has been omitted in the main curve. Details of the curve including oxygen are shown in the inset [50].

tributing to these peaks is rather complex and only the main features will be outlined here. The first CO_2 peak appearing below the peak of CO is the result of direct reaction of CO with oxygen from the support (true oxygen-storage) while the second contribution, which appears under the peak of oxygen, depends strongly on surface area and temperature and is probably due to desorption of CO_2 in the presence of oxygen or to reaction between adsorbed CO and O_2. Possible participation of the CO disproportionation reaction ($2CO \leftrightarrow C + CO_2$) in the dynamics of oxygen-storage cannot be excluded at this stage, especially for ceria. CO_2 evolution in the case depicted in Fig. 7 starts at ca. 550 K, reaching complete conversion at around 700 K. The first component reaches a steady-state value at ca. 750 K while the second component shows a maximum of intensity at around 640 K. The temperature at which 50% conversion of CO is observed was used to measure the relative activity of the different catalysts. It is important to stress here that this method allows a quantification of the contribution of true oxygen-storage to overall activity as a function of temperature and under dynamic conditions typical of auto exhaust catalysis.

Fig. 8 shows the TP dynamic reaction profile of CO_2 evolution from HSA and aged, low-surface area (LSA) ceria and $Ce_{0.5}Zr_{0.5}O_2$ [51]. The region characteristic of each CO_2 component is indicated with 1

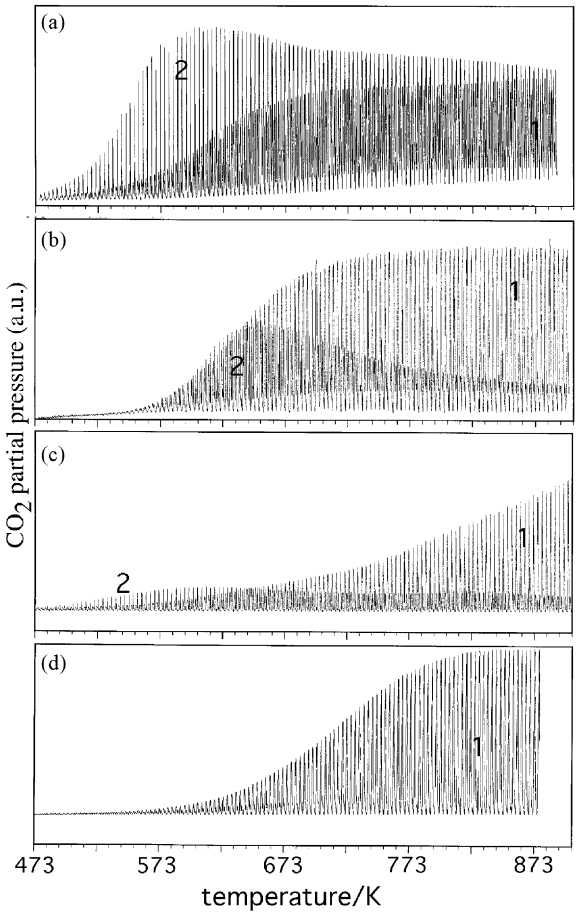

Fig. 8. Details of CO_2 formation (components 1 and 2) in TP CO oxidation of HSA ceria (a), $Ce_{0.5}Zr_{0.5}O_2$ (b), LSA ceria (c) and $Ce_{0.5}Zr_{0.5}O_2$ (d) [51].

and 2. The following considerations emerge from this analysis: HSA ceria is more active than ceria-zirconia in terms of overall CO_2 formation, activity starting at ca. 470 K (530 K for ceria-zirconia), but analysis of CO_2 formation shows that true oxygen-storage (component 1) is in a minority in ceria. A large fraction results from surface reaction between CO and oxygen. This explains why with aged catalysts a dramatically different situation exists. Only component 1 is observed (a residual surface activity persists on ceria) and ceria-zirconia is far more active than ceria. A substantial difference exists between the activity of catalysts subjected to reaction under stationary and dynamic/cycled feedstream composition. In the first case, activity depends mainly on surface area and exposed surface redox centers (i.e. Ce ions) while under cycled conditions structural features of the material becomes more important. Surface area is still an important parameter under dynamic conditions but as the oscillation frequency decreases, the mobility of oxygen through the bulk may compensate for loss of surface area. Therefore, at low oscillation frequency, aged samples of ceria-zirconia perform better than ceria, in agreement with their greater ability to use bulk oxygen anions for oxidation [52].

A similar TP dynamic analysis was recently developed by Bernal et al. [46]. The experimental method consists of injecting pulses of O_2 in an He stream with an interval of 10 s while linearly increasing temperature. The O_2 content is measured with a TCD detector at the outlet of the reactor. In this way, it is possible to rapidly evaluate the oxygen buffering capacity of

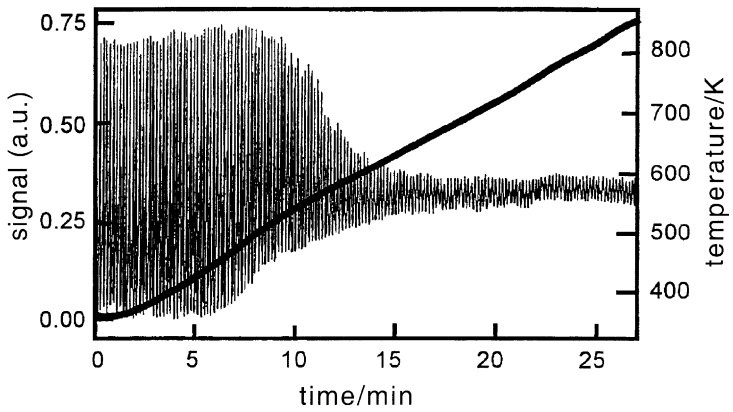

Fig. 9. TCD detector signal for experiment conducted on $Ce_{0.8}Tb_{0.2}O_2$ catalyst [46].

a catalyst, that is the ability to attenuate the oxygen pressure induced by the pulses as a function of temperature (Fig. 9). It was applied to the characterization of oxygen-storage behavior of ceria-terbia and ceria-zirconia catalysts and results obtained are in good agreement with those obtained with TPR [53].

References

[1] J.L. Falconer, J.A. Schwarz, Catal. Rev. Sci. Eng. 25 (1983) 141.
[2] J.L. Lemaitre, in: F. Delannay (Ed.), Characterization of Heterogeneous Catalysts, Marcel Dekker, New York, Chapter 2, 1984.
[3] A. Jones, B. McNicol, Temperature-Programmed Reduction for Solid Material Characterization, Marcel Dekker, New York, 1986.
[4] S. Bhatia, J. Beltramini, D.D. Do, Catal. Today 7 (1990) 308.
[5] R.J. Cvetanovic, Y. Amenomiya, Adv. Catal. 17 (1967) 67.
[6] E.E. Ibok, D.F. Ollis, J. Catal. 66 (1980) 391.
[7] R.J. Gorte, J. Catal. 75 (1982) 164.
[8] E. Tronconi, P. Forzatti, J. Catal. 93 (1985) 197.
[9] D.A.M. Monti, A. Baiker, J. Catal. 83 (1983) 323.
[10] R.J. Farrauto, R.M. Heck, Catal. Today 51 (1999) 351.
[11] M. Ricken, J. Nölting, I. Riess, J. Solid State Chem. 54 (1984) 89.
[12] J. Zhang, Z.C. Kang, L. Eyring, J. Alloys Comp. 192 (1993) 57.
[13] P. Loof, B. Kasemo, S. Andersson, A. Frestad, J. Catal. 130 (1991) 181.
[14] T. Jin, T. Okuhara, G.J. Mains, J.M. White, J. Phys. Chem. 91 (1987) 3310.
[15] C. Padeste, N.W. Cant, D.L. Trimm, Catal. Lett. 18 (1993) 305.
[16] F. Roozeboom, M.C. Mittlemeijer-Hazeleger, J.A. Moulijn, J. Medema, V.H.J. de Beer, P.J. Gellings, J. Phys. Chem. 84 (1980) 2783.
[17] H.C. Yao, Y.F.Y. Yao, J. Catal. 86 (1984) 254.
[18] V. Perrichon, A. Laachir, G. Bergeret, R. Frety, L. Tournayan, O. Touret, J. Chem. Soc., Faraday Trans. 90 (1994) 773.
[19] A. Trovarelli, G. Dolcetti, C. de Leitenburg, J. Kaspar, P. Finetti, A. Santoni, J. Chem. Soc., Faraday Trans. 88 (1992) 1311.
[20] S. Bernal, J.J. Calvino, G.A. Cifredo, A. Laachir, V. Perrichon, J.M. Herrmann, Langmuir 10 (1994) 717.
[21] C. de Leitenburg, A. Trovarelli, J. Kaspar, J. Catal. 166 (1997) 98.
[22] F. Giordano, A. Trovarelli, C. de Leitenburg, M. Giona, J. Catal. 193 (2000) 273.
[23] F. Giordano, A. Trovarelli, C. de Leitenburg, G. Dolcetti, M. Giona, Ind. Eng. Chem. Res. 40 (2001) 4828.
[24] J. Kaspar, P. Fornasiero, M. Graziani, Catal. Today 50 (1999) 285.
[25] P. Fornasiero, R. Di Monte, G. Ranga Rao, J. Kaspar, S. Meriani, A. Trovarelli, M. Graziani, J. Catal. 151 (1995) 168.
[26] F.M.Z. Zotin, L. Tournayan, J. Varlaud, V. Perrichon, R. Frety, Appl. Catal. A 98 (1993) 99.
[27] N. Hickey, P. Fornasiero, R. Di Monte, J. Kaspar, M. Graziani, G. Dolcetti, Catal. Lett. 72 (2001) 45.
[28] S. Bernal, J.J. Calvino, J.M. Gatica, C. López Cartes, J.M. Pintado, in: A. Trovarelli (Ed.), Catalysis by Ceria and Related Materials Catalytic Science Series, vol. 2, Imperial College Press, London, Chapter 4, 2002, pp. 85–168.
[29] A. Trovarelli, Catal. Rev. Sci. Eng. 38 (1996) 439.
[30] S. Bernal, J.J. Calvino, G.A. Cifredo, J.M. Gatica, J.A. Pérez Omil, J.M. Pintado, J. Chem. Soc., Faraday Trans. 89 (1993) 3499.
[31] V. Perrichon, A. Laachir, S. Abouarnadasse, O. Touret, G. Blanchard, Appl. Catal. A 129 (1995) 69.
[32] L.A. Bruce, M. Hoang, A.E. Hughes, T.W. Turney, Appl. Catal. A 134 (1996) 351.
[33] J.H. Wang, T.O. Mason, Zeitschrift Phys. Chem. 207 (1998) 21.
[34] S. Bernal, J.J. Calvino, G.A. Cifredo, J.M. Rodriguez-Izquierdo, J. Phys. Chem. 99 (1995) 11794.
[35] K. Sohlberg, S.T. Pantelides, S.J. Pennycook, J. Am. Chem. Soc. 123 (2001) 6609.
[36] A. Badri, C. Binet, J.C. Lavalley, J. Chem. Soc., Faraday Trans. 96 (1996) 4669.
[37] C. Lamonier, G. Wrobel, J.P. Bonnelle, J. Mater. Chem. 4 (1994) 1927.
[38] J.L.G. Fierro, J. Soria, J. Sanz, J.M. Rojo, J. Solid State Chem. 66 (1987) 154.
[39] P. Fornasiero, N. Hickey, J. Kaspar, T. Montini, M. Graziani, J. Catal. 189 (2000) 339.
[40] E. Rocchini, M. Vicario, J. Llorca, C. de Leitenburg, G. Dolcetti, A. Trovarelli, J. Catal. 211 (2002) 407.
[41] A. Badri, C. Binet, J.C. Lavalley, J. Chem. Soc., Faraday Trans. 92 (1996) 4669.
[42] F. Zimmer, A. Tschope, R. Birringer, J. Catal. 205 (2002) 339.
[43] A. Trovarelli, F. Zamar, J. Llorca, C. de Leitenburg, G. Dolcetti, J.T. Kiss, J. Catal. 169 (1997) 490.
[44] C.E. Hori, H. Permana, Ng.K.Y. Simon, A. Brenner, K. More, K.M. Rahmoeller, D. Belton, Appl. Catal. B 16 (1998) 105.
[45] H.W. Jen, G.W. Graham, W. Chun, R.W. McCabe, J.P. Cuif, S.E. Deutsch, O. Touret, Catal. Today 50 (1999) 309.
[46] S. Bernal, G. Blanco, M.A. Cauqui, P. Corchado, J.M. Pintado, J.M. Rodriguez Izquierdo, Chem. Commun. 1545 (1997).
[47] A. Holmgren, B. Andersson, D. Duprez, Appl. Catal. B 22 (1999) 215.
[48] Y. Madier, C. Descorme, A.M. Le Govic, D. Duprez, J. Phys. Chem. B 103 (1999) 10999.
[49] D. Duprez, C. Descorme, T. Birchem, E. Rohart, Top. Catal. 16/17 (2001) 49.
[50] M. Boaro, C. de Leitenburg, G. Dolcetti, A. Trovarelli, M. Graziani, Top. Catal. 16/17 (2001) 299.
[51] M. Boaro, et al., to be submitted.
[52] M. Boaro, C. de Leitenburg, G. Dolcetti, A. Trovarelli, J. Catal. 193 (2000) 338.
[53] H. Vidal, J. Kaspar, M. Pijolat, G. Colon, S. Bernal, A. Cordon, V. Perrichon, F. Fally, Appl. Catal. B 27 (2000) 49.